



Water Resources Research®

RESEARCH ARTICLE

10.1029/2021WR031745

Key Points:

- A Bayesian dynamic linear model is developed to detect pipe burst by modeling flow time series and monitoring outliers
- The model naturally accommodates nonlinear associations between flow and predictors (e.g., pressure, temperature)
- Non-stationarity of the flow time series is naturally accounted for through the dynamic structure of the parameters in the model

Supporting Information:

Supporting Information may be found in the online version of this article.

Correspondence to:

A. M. Schmidt,
alexandra.schmidt@mcgill.ca

Citation:

Henriques-Silva, R., Duchesne, S., St-Gelais, N. F., Saran, N., & Schmidt, A. M. (2023). On-line warning system for pipe burst using Bayesian dynamic linear models. *Water Resources Research*, 59, e2021WR031745. <https://doi.org/10.1029/2021WR031745>

Received 13 DEC 2021
Accepted 1 MAR 2023
Corrected 20 APR 2023

This article was corrected on 20 APR 2023. See the end of the full text for details.

Author Contributions:

Conceptualization: Renato Henriques-Silva, Sophie Duchesne, Nicolas Fortin St-Gelais, Naysan Saran, Alexandra M. Schmidt
Data curation: Renato Henriques-Silva
Formal analysis: Renato Henriques-Silva
Funding acquisition: Nicolas Fortin St-Gelais, Naysan Saran, Alexandra M. Schmidt

© 2023 The Authors.

This is an open access article under the terms of the [Creative Commons Attribution-NonCommercial License](#), which permits use, distribution and reproduction in any medium, provided the original work is properly cited and is not used for commercial purposes.

On-Line Warning System for Pipe Burst Using Bayesian Dynamic Linear Models

Renato Henriques-Silva¹ , Sophie Duchesne² , Nicolas Fortin St-Gelais³, Naysan Saran³, and Alexandra M. Schmidt¹ 

¹Department of Epidemiology, Biostatistics and Occupational Health, McGill University, Montreal, QC, Canada, ²Research Centre on Water, Earth, and the Environment, Institut National de La Recherche Scientifique (INRS), Quebec City, QC, Canada, ³CANN Forecast, Montreal, QC, Canada

Abstract Pipe breaks are a recurrent problem in water distribution networks and detecting them quickly is crucial to minimize the economic and environmental costs for municipalities. This study presents a burst detection methodology applying Bayesian dynamic linear models (DLMs) on water flow time series combined with an outlier monitoring tool. The model is used to characterize the actual flow and, for each time, a one-step ahead forecast distribution is obtained recursively before moving onto the next observation. The outlier detection method consists of comparing the main model with an alternative one wherein the mean flow is shifted to a higher value (as bursts tend to increase flow) to evaluate which model best fit the observed data. If the alternative model is favored, a burst alarm is issued. To verify the performance of this approach, the DLM and monitoring tool were applied on 2 yr of flow data from two district meter areas (DMAs) in Halifax (Canada), and a historical break data set is used to assess model accuracy. The model was able to detect up to 75% and 71.2% of the pipe breaks, with a false alarm rate of 5.15% and 12% in the first and second DMA, respectively. Finally, the proposed model allows for straightforward interpretation of model parameters, nonlinear relationship between flow and predictors of interest, naturally describes the uncertainty for future predictions, can easily accommodate missing values and can be tuned to maximize break detection or minimize false alarm rates to adapt to specific objectives of water infrastructure managers.

1. Introduction

The distribution of drinking water is an indispensable service provided by municipalities and water utilities. Given the rapid population growth and consequent increasing pressure on water resources, it is fundamental for cities to optimize the use of existing water supplies. Optimization of water use includes, among other aspects, minimizing water loss due to leaks and bursts in the system. Pipe breaks are a recurrent issue in aging water distribution systems (WDSs) and common causes of this problem are pipe deterioration (i.e., corrosion), weather (e.g., extreme cold, drought events), suboptimal installation practices, excessive pressure and/or excessive pressure fluctuation (Rezaei et al., 2015). Yet, despite continuing efforts to cope with this problem, unacceptable amounts of water continue to be lost across WDS worldwide. It has been estimated that more than 32 billion cubic meters/year of treated water are lost in water distribution networks across the world due to leaks and burst in pipes (Kingdon et al., 2006). More alarmingly, this situation is not getting any better. For instance, according to a recent report, the overall failure rate of pipes across the United States and Canada have increased by 27% from 2012 to 2018 (Folkman, 2018). These failures can cause many problems such as lower level of pressure heads offered to customers, floods, water contamination (Sadiq et al., 2006), service interruption to the end user (Yamijala et al., 2009) as well as revenue loss for water utilities. Hence, rapid burst detection is necessary for water utilities to intervene early and minimize these various impacts.

Over the past two decades, many methods have been developed to decrease the time between a burst and its detection (Li et al., 2015). Hardware-based methods use highly specialized equipment such as leak noise loggers, gas injection, and ground penetrating radar (Nakhkash & Mahmood-Zadeh, 2004) are currently the most accurate in detecting and locating leaks and bursts (Puust et al., 2010). However, such methods are generally expensive, labor-intensive and/or require interrupting the pipeline operation during usage (Romano et al., 2014). Recent development in hydraulic sensor technology and on-line data acquisition systems (SCADA; Supervisory Control and Data Acquisition) have fostered the emergence of various types of software-based methods relying on hydraulic modeling, statistical analysis, and artificial intelligence (e.g., Mounce et al., 2010; Romano et al., 2014;

Investigation: Renato Henriques-Silva, Alexandra M. Schmidt

Methodology: Renato Henriques-Silva, Sophie Duchesne, Alexandra M. Schmidt

Project Administration: Renato Henriques-Silva, Nicolas Fortin St-Gelais, Alexandra M. Schmidt

Resources: Naysan Saran, Alexandra M. Schmidt

Software: Renato Henriques-Silva

Supervision: Sophie Duchesne, Alexandra M. Schmidt

Validation: Renato Henriques-Silva, Sophie Duchesne, Nicolas Fortin St-Gelais, Alexandra M. Schmidt

Visualization: Renato Henriques-Silva

Writing – original draft: Renato

Henriques-Silva

Writing – review & editing: Renato Henriques-Silva, Sophie Duchesne, Nicolas Fortin St-Gelais, Naysan Saran, Alexandra M. Schmidt

Wang et al., 2020; Ye & Fenner, 2011) such as artificial neural networks (ANNs, Mounce et al., 2002), deep learning (Wang et al., 2020; Zhou et al., 2019) and support vector machines (Mounce et al., 2011), among others. Software-based detection methods can be classified as transient-state and non-transient methods (Wan et al., 2022). The main idea behind both these methods is that bursts and leaks will leave “signatures” in hydraulic variables measurements (e.g., flow, pressure). In the case of transient-state methods, breaks are detected by analyzing the transient signal due to sudden changes in pressure inside pipes where a break occurs (e.g., Navarro-Díaz et al., 2022). Non-transient methods are based on algorithms that are trained to detect deviations from the usual patterns of hydraulic variables measurements during a burst event (Bakker et al., 2014; Y. Wu & Liu, 2017; Ye & Fenner, 2011). This can be done either by comparing the hydraulic measurements (e.g., flow, pressure) to values predicted by hydraulic simulation models (hydraulic model-based methods; see e.g., Ma et al., 2022) or by applying data mining algorithms or statistical analysis to the acquired data to distinguish abnormal values from the usual patterns that may be caused by events such as breaks (data-drive methods). As an alternative, Geelen et al. (2019) suggested analyzing sudden changes in pressure measurements instead of deviations from the usual pattern. Recent reviews on software-based methods for water pipe break detection are provided by Hu et al. (2021) and Wan et al. (2022).

In days without any special events or issues (e.g., pipe burst, fire hydrant use), hydraulic data follows a specific periodicity (daily, weekly, Figure 1) driven by consuming patterns of end users (Y. Wu & Liu, 2017). A typical daily pattern is characterized by a flow peak during mornings and minimum flow at night (see Figure 1d). However, water distribution networks do not operate under ideal conditions all the time. Hydraulic monitoring may produce missing or false data due to problems with sensors or issues with the communication between sensors and data loggers (Quevedo et al., 2010; Y. Wu & Liu, 2017). Moreover, water demand varies due to many different factors (e.g., weather, occurrence of festivals, big consumers, maintenance work, and seasons), meaning that the time series of flow is non-stationary (Y. Wu & Liu, 2017). Hydraulic monitoring and outlier detection should thus be conducted with methods that do not assume stationarity such as gradient boosted trees, random forests, and ANN, among others (Wan et al., 2022). Jian et al. (2022) suggested the use of convolutional neural networks to build pattern recognition and use it to flag leaks and bursts. While successful, these approaches require a large amount of data, may be computationally intensive and/or have poor scalability. In the present study, it is proposed the use of Bayesian dynamic linear models (DLMs), which can also accommodate non-stationarity and has a very efficient (and fast) inference procedure when approximated with the principle of discount factors (see further below). Moreover, the DLM goes beyond a simple time series model that use only historical water flow as the only input and can explore the complex effects of various external factors that affect water flow in a water distribution network. This approach has been used in engineering, epidemiology, economics, to mention a few examples. Examples for applications of DLM are diverse: modeling electric load curves (Migon & Alves, 2013), hydrological forecasting (Ciupak et al., 2015; Ravines et al., 2008) and forecasting of epidemiologic time series for public health surveillance (Nobre et al., 2001). See Schmidt and Lopes (2019) for a recent review.

To be able to distinguish an abnormal event (e.g., burst) from a usual water flow pattern, algorithms generally rely on error thresholds. The value of these thresholds should not be static as water flow intensity vary over time (daily, weekly, yearly; Figure 1). The size and composition of district meter areas (DMA) also affects water flow. For instance, the presence of a large industrial consumer may have considerable influence in water flow patterns. Thus, a threshold used for outlier detection in one DMA may not be appropriate for a different DMA. Ye and Fenner (2014) proposed a Kalman filter algorithm with a method to generate thresholds based on mean and standard deviation of historical residuals that would thus be adaptable to different WDSs. However, the Kalman filter proposed by Ye and Fenner (2014) only assumes a time varying level. The problem with this approach is that there might be structures left in the residual (e.g., cycles, association with regressors) that are not related to bursts. In contrast, the Bayesian DLM not only can include time-varying level, slope, and seasonality but also external factors such as temperature and dummy variables associated with the days of the week and holidays. Given that the coefficients associated with these variables change smoothly with time, nonlinear relationships are easily accommodated. Moreover, it analyzes observations in real time, updating the posterior distribution of the parameters as new observations are available. This allows the model to adapt over time to changes in the WDS that may affect the flow time series. Finally, outlier detection in water flow time series is proposed by continuously evaluating the model predictive performance using a monitoring approach. Model monitoring within the DLM framework has been applied extensively in the field of structural health monitoring and examples can be

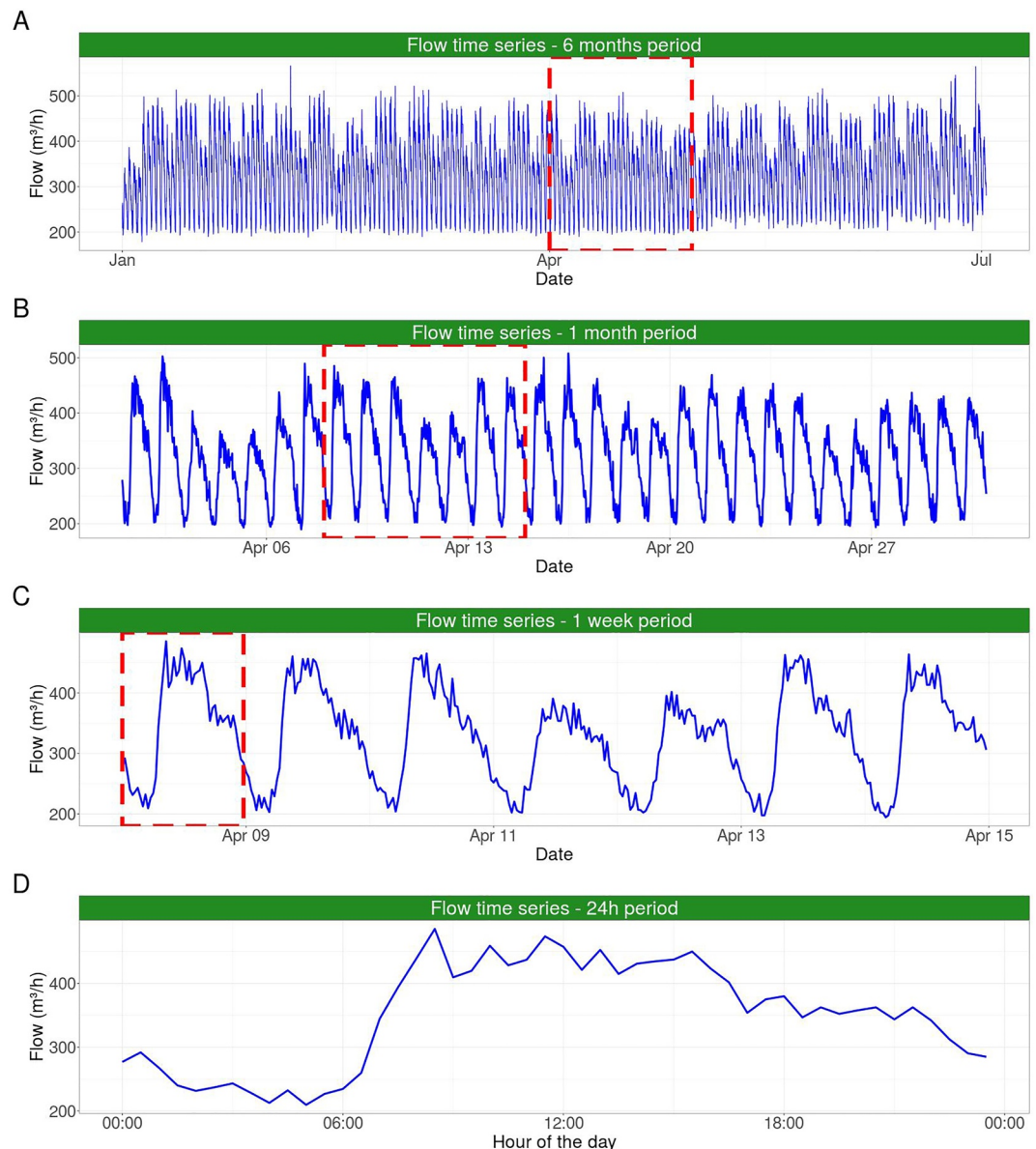


Figure 1. Temporal structure of the flow time-series. (a) Six-month flow time series (01 January to 30 June 2015); (b) 1-month flow time series (April 2015); (c) 1-week flow time series (8–14 April 2015), (d) 24 hr flow time series (8 April 2015). The red dashed quadrant represents the progressive zooming of the time series from panels (a–d).

found for gas turbines (Lipowsky et al., 2010), bridges (Liu & Fan, 2020), and even wheels in high-speed trains (Wang, Ni, & Wang, 2020). However, to the best of our knowledge, there are no studies evaluating its potential to monitor water distribution networks in the context of pipe burst detection.

The objective of this study is to propose and assess the performance of a Bayesian DLM coupled with a model monitoring approach for burst detection. The proposed model is fitted to a real flow data set from two DMAs from Halifax, Canada. The novelty of the proposed approach relies, first, in the application of a Bayesian DLM combined with the use of the principle of discount factors (Migon & Alves, 2013) to estimate the system variance. The latter speeds up the model inference compared to stochastic simulations that are commonly applied for this task. Second, the monitoring tool using the Bayes factor is applied to detect pipe bursts. Finally, we demonstrate how the interpretation of the model coefficients can be used by practitioners to gain valuable insights into the modeled system. In Section 2.1, the data sets used in the study are presented along with the description of data cleaning and transformation procedures. Section 2.2 describes the Bayesian univariate DLM, with a detailed

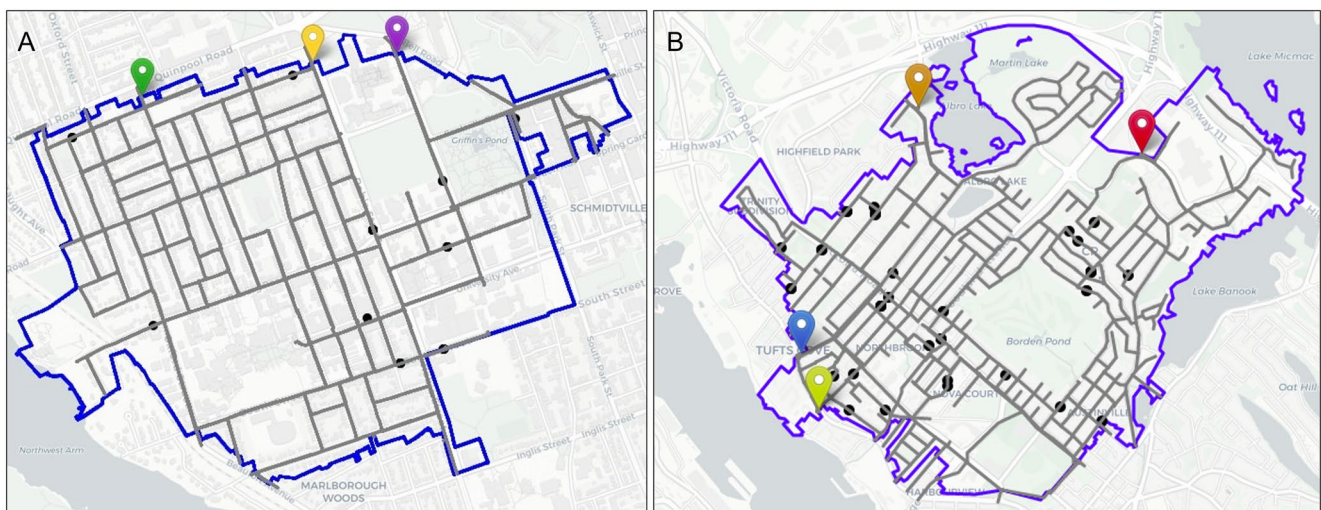


Figure 2. The pipeline network (gray lines), the layout of flow meters (represented by location markers) and the pipe burst location (black solid circles) for the two DMAs. (a) DMA 1: The summary statistics of inlet flow meters 1, 2, and 3 (green, yellow, and violet, respectively) are detailed in Table 1. The pressure meter is installed at the same location of inlet flow meter 2 (yellow location marker). (b) DMA 2: The summary statistics of inlet flow meters 4 and 5 (orange and red, respectively), and outlet flow meters 1 and 2 (blue and light green, respectively) are detailed in Table 1. The pressure meter for this district meter area (DMA) is installed at the same location of inlet flow meter 5 (red location marker).

description of the filtering and forecasting equations. In Section 2.3, an outlier detection method is proposed to detect pipe breaks in water flow time series. Section 3 describes the results obtained when the model is fitted to the flow data sets and discusses the performance and applicability of the proposed methodology, while the conclusions of this study are presented in Section 4.

2. Methods

2.1. Data

2.1.1. Data Set

We used water flow data sets from Halifax Water (the water utility from the city of Halifax, Canada) for two of their DMA (Figure 2). The first DMA is composed mostly of single residential units, and includes a university, two hospitals, a busy commercial district and a small number of high-rise residential buildings. It has 25 km of water mains, 1,900 service connections and an average pressure of 50 psi (~ 344.7 kPa). The DMA has three feeding points, all monitored by flow meters, and no outlets (see Figure 2a). The second DMA (Figure 2b) is a predominantly residential zone, with a few commercial areas (one large mall, a couple of smaller commercial complexes) and a small number of multi-residential and office buildings. It is also larger than the first one, composed of 59 km of water mains and 3,800 service connections with an average pressure of 66.7 psi (~ 459.9 kPa). In addition to the two feeding points, this DMA has two outlets, all monitored by flow meters. The two data sets contain the flow measurements (m^3/h) at 30 min intervals between 1 January 2015 and 31 December 2016 for all flowmeters. They also contain water pressure (psi) measured at similar frequency and date range from a single pressure sensor that is paired with one of the flow meters.

Summary statistics for the flow and pressure meters are presented in Table 1. Temperature data was gathered from *Halifax Stanfield INT'L A* meteorological station, which was obtained from Environment Canada's website (https://climat.meteo.gc.ca/index_e.html). This data is composed of hourly temperature measurements (in Celsius) that were restrained to the same date range as the hydraulic data. Hourly temperatures ranged from -21.7°C during the coldest day in winter up to $+30.0^\circ\text{C}$ during the warmest day in summer, with a mean value of 6.95°C for the entire time series. Halifax Water also provided a historical break data set, containing the dates for breaks that occurred in the water distribution network of the studied DMA (black solid circles in Figure 2). A total of 8 and 28 breaks occurred during the studied period in DMAs 1 and 2, respectively, and these were used to evaluate the performance of the monitoring tool developed within the DLM framework..

Table 1
Summary Statistics of the Raw Data From Flow and Pressure Sensors

DMA	Sensor	Max	Min	Median	Mean	SD	Missing	Repeated (false)	False + missing
1	Inlet Flow meter 1 (m^3/h)	1,004.22	4.70	203.62	204.37	50.4	11	707	2.04%
1	Inlet Flow meter 2 (m^3/h)	299.83	12.54	52.92	53.47	13.7	10	1,925	5.51%
1	Inlet Flow meter 3 (m^3/h)	381.46	5.56	77.64	78.44	17.9	10	1,079	3.10%
1	Inlet Pressure meter 1 (psi)	63.35	22.06	50.97	50.93	2.04	10	485	1.41%
2	Inlet Flow meter 4 (m^3/h)	545.5	0.031	114.12	111.23	53.3	6	21	0.07%
2	Inlet Flow meter 5 (m^3/h)	317.60	0.0033	97.23	88.30	31.2	5	21	0.07%
2	Outlet Flow meter 1 (m^3/h)	183.72	0.041	0.94	3.80	8.9	7	0	0.02%
2	Outlet Flow meter 2 (m^3/h)	250.01	0.0051	47.01	40.32	20.9	25	360	1.10%
2	Inlet Pressure meter 2 (psi)	82.2	0.1	70.21	69.27	2.6	5	21	0.07%

Note. The total number of measurements (N) per meter is 35,088. Max, maximum value; Min, minimum value, SD, standard deviation; Missing, number of missing values; Repeated, number of repeated values in sequence (considered as false). False + Missing, percentage of unrecorded or false data from each sensor.

2.1.2. Data Cleaning and Wrangling

Some sensors presented a few missing or false data due to operation problems in the communication system between the data logger and the sensors. Flow (or pressure) sensor readings with repeated values on three or more consecutive measurements were considered to be false data (see Table 1). While there is a chance that the variable measured presents the same value over three time steps, it is extremely unlikely given the precision of the readings, and thus those values were treated as missing values in the model. The total amount of false and missing data per sensor ranged from 0.07% up to 5.51% of the total number of measurements (Table 1). To decrease the complexity of the model, the 30 min data from pressure and flow were grouped into hours by computing the average of two consecutive observations in each hour. If one of the two values in 1 hr was missing, then the other was taken to represent the measurement at that hour. Then, the time series of total flow was created by adding up the values from the inlet flow meters and subtracting the values from the outlet flow meters (in case of DMA 2) at each time step. However, in any time step where one flow meter had a missing value, the total flow for that time step was considered as missing, regardless of whether the values of other flow meters were validated. Here, total flow represents the total water demand from the DMA.

The final flow time series contained 17,544 hourly measurements, in which 902 (5.14%) and 175 (1%) were considered as missing following the above-mentioned criteria in DMAs 1 and 2, respectively. Accounting for missing values within a Bayesian framework is straightforward: the model parameters are not updated when encountering them in the time series (West & Harrison, 1997). More details on how the DLM deals with missing data is presented in Section 2.2.2. Finally, after cleaning, flow values were log-transformed to have an approximate normal distribution. The model forecast was transformed back to the original scale for better interpretability.

Note that the pressure time series also presented some missing values (Table 1). To deal with missing values in water pressure, a DLM similar to the one described for the flow time-series was used to estimate these missing records. All components from the original DLM were used (i.e., trend, dummy variables, temperature, and the auto-regressive component). Note that flow was not included as a predictor to avoid circularity. All missing or false observations in the original pressure time series were substituted with the estimated values from this model. More details are presented in the “Results and Discussion” section.

2.1.3. Synthetic Bursts

Given that the historical break data set contains only the dates of the pipe bursts, the detection time could not be evaluated. To overcome this issue, 16 scenarios were created wherein synthetic outliers were added to the initial flow time series of 30 dates selected at random, excluding dates with real bursts or with missing flow values from the selection. Each scenario represented a combination of four different starting timestamps where the outliers would be added and three types of bursts size. The starting timestamps were 2:00 a.m., 8:00 a.m., 2:00 p.m., and 8:00 p.m., which aimed at capturing the peaks and troughs in water demand (Wang et al., 2020). Pipe bursts of different sizes were created by adding outliers that were equivalent to 8%, 10%, 12%, or 15% of the average flow

of the selected date to the actual flow of these timestamps. Finally, for each synthetic burst, 10 outliers (representing 10 hr in the flow data set used in this study) were added, starting at the above-mentioned timestamps (for example, from 2:00 a.m. to 11:00 a.m., from 8:00 a.m. to 5:00 p.m. and so on).

2.2. Bayesian DLM

One can think of a DLM as a linear regression model where the regression coefficients are allowed to vary smoothly over time. These models can capture time series features such as trend, seasonality, and regression associations (Petris et al., 2009). DLMs are a specific case of a broad class of models called state-space models (Petris et al., 2009) wherein an observable/measurable phenomenon (y_t) at a given time t depends on an underlying unobserved (latent) state (θ_t) of a particular system. The DLM allows the modeler to update their beliefs about the current value of this unobserved state each time a new observation is made using an associated algorithm named the Kalman filter. In the present study, separate daily DLMs were built for each hour (h) of the day (t), resulting in a total of 24 univariate dynamic models. Each hour of the day shows a particular flow pattern and this approach allows to capture this temporal structure, in addition to be much faster to fit than multivariate models (Migon & Alves, 2013). Although other authors have modeled flow at higher resolutions (e.g., 15 min intervals; Ye & Fenner, 2011), the historical break data set used in this study only provided information on a day of the break, hence dividing the time series into finer resolution series would not make a difference for performance analysis. The univariate DLM is composed of two main equations: the observation equation (Equation 1), which decomposes the observed time series as the sum of some specific components and a white noise random variable, and the system equation (Equation 2), which describes how the components of the system evolve smoothly over time. More specifically, let $y_{t,h}$ be the flow time series observed at hour h of day t , then the DLM is defined as follows:

$$y_{t,h} = F_{t,h}^T \theta_{t,h} + v_{t,h}, v_{t,h} \sim N[0, V_{t,h}] \quad (1)$$

$$\theta_{t,h} = G\theta_{t-1,h} + w_{t,h}, w_{t,h} \sim N[0, W_{t,h}] \quad (2)$$

where $\theta_{t,h}$ is a p -dimensional unknown state parameter vector at hour h and day t . In other words, the vector $\theta_{t,h}$ contains the p coefficients of the different DLM components (e.g., level, slope, predictors, dummies, and auto regressive component, see Section 2.2.1). $F_{t,h}$ is a p -dimensional column-vector that contains known structures (e.g., level, slope, seasonality, predictors) for day t and hour h , and G is a $p \times p$ matrix of known quantities describing the state evolution (in this study it is constant over time, although it can accommodate changes over time). Finally, $v_{t,h}$ is a Gaussian random variable, representing measurement error, with mean 0 and variance $V_{t,h}$; and $w_{t,h}$, on the other hand, is p -dimensional random vector, which captures the errors of the evolution equation of the parameters, it follows a zero mean, multivariate normal distribution with covariance matrix $W_{t,h}$. The errors $v_{t,h}$ and $w_{t,h}$ are mutually independent as well as independent across time. To simplify the notation, from now on the index h is dropped and t is used to refer to time.

2.2.1. Model Components

The DLM decomposes an observation at a given time step t as a combination of elementary components, each describing different features of the time series, such as trend, seasonality, and association with predictors.

Trends in DLM are commonly represented by second order polynomials (Pole et al., 1994), which describe either growth or decline in the system level. The state vector representing this component $\theta_{1t} = (\mu_{1,t}, \mu_{2,t})^T$ comprises two components: the level and the slope. The DLM trend is represented as follows:

$$F_{1t} = (1, 0)^T \text{ and } G_1 = \begin{pmatrix} 1 & 1 \\ 0 & 1 \end{pmatrix}$$

The state vector from the second component $\theta_{2t} = (\beta_{1,t}, \beta_{2,t}, \beta_{3,t})^T$ includes three predictors, one representing the auto-regressive order 1 (y_{t-1}) coefficient ($\beta_{1,t}$), and the two others representing the coefficients ($\beta_{2,t}$) and ($\beta_{3,t}$), for pressure (Press _{t}) and temperature (Temp _{t}), respectively. This block is defined as follows:

$$F_{2t} = (y_{t-1}, \text{Press}_t, \text{Temp}_t)^T \text{ and } G_2 = I_3$$

where I_3 denotes the 3-dimensional identity matrix.

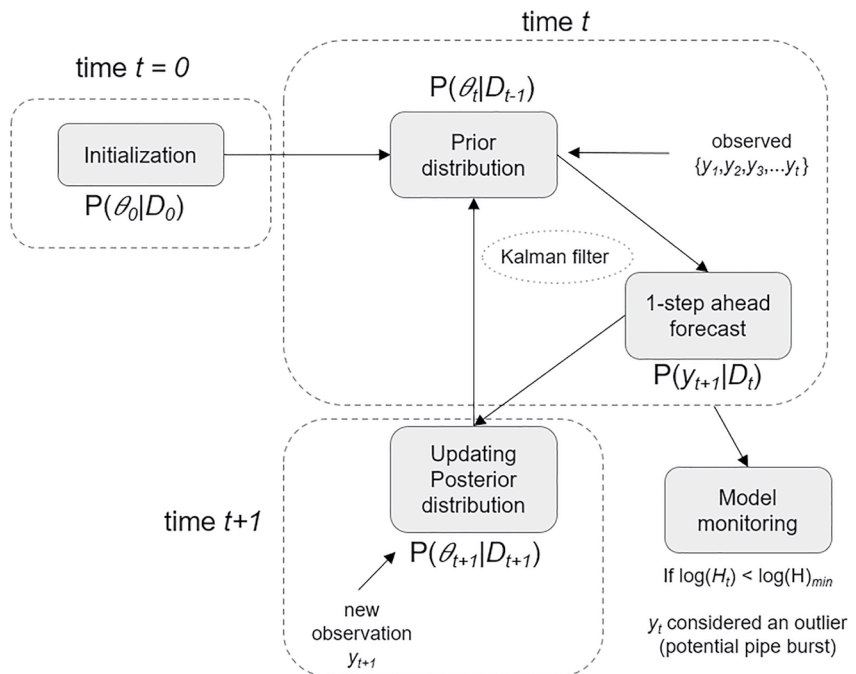


Figure 3. Flowchart for the dynamic linear model initialization and updating.

Water demand varies between weekdays and weekends/holidays (see Figure 1) and dummy variables were included to consider this variation. The third component describes the effect of these two dummy variables $d_{1,t}$ and $d_{2,t}$, where weekends are represented by ($d_{1,t} = 0, d_{2,t} = 1$) and workdays by ($d_{1,t} = 1, d_{2,t} = 0$), with the exception of Monday which was defined as the baseline for the dummies ($d_{1,t} = 0, d_{2,t} = 0$). Christmas, Thanksgiving, and other holidays during 2015 and 2016 were considered as weekends ($d_{1,t} = 0, d_{2,t} = 1$) in the dummy variables. The state vector for the third component $\theta_{3t} = (\gamma_{1,t}, \gamma_{2,t})^T$ contains the coefficients for these dummy variables. This block is defined as follows:

$$F_{3t} = (d_{1t}, d_{2t})^T \text{ and } G_3 = I_2$$

where I_2 is the 2-dimensional identity matrix. Finally, these three components are then combined using the superposition principle (West & Harrison, 1997) into the final design and evolution matrices:

$$F = (F_{1t}^T, F_{2t}^T, F_{3t}^T)^T \text{ and } G = \begin{bmatrix} G_1 & 0 & 0 \\ 0 & G_2 & 0 \\ 0 & 0 & G_3 \end{bmatrix}$$

2.2.2. Bayesian Forecasting

Bayesian inference is recursive by nature where model parameters are updated as new observations are added, making it a natural fit for time series analysis (Petrus et al., 2009). Bayesian forecasting in DLMs is controlled by a series of equations that are commonly known as the Kalman filter algorithm, which are described below. They present univariate models for each hour of the day, but h is omitted for clearer readability. The model is built under the assumption of an unknown constant variance, such that $V_t = V$ for all time steps t and that the covariance structure of the evolution equation is known through the use of discount factors. A diagram of the model is presented in Figure 3.

1. Model initialization

The joint prior distribution for the initial state parameter vector θ_0 and the observational variance V is a normal inverse-gamma ($N - IG$) distribution, that is,

$$\theta_0, V \sim N - IG\left(m_0, C_0, \frac{n_0}{2}, \frac{n_0 S_0}{2}\right)$$

where $n_0 > 0$ is the prior degrees of freedom and S_0 is a prior point estimate of the observational variance V , $m_0 (p \times 1)$ and $C_0 (p \times p)$ are the prior mean and variance ($C_0 = 10^2 I_p$) of the state parameter θ_0 , conditional on the observational variance V ; I_p denotes a p -dimensional identity matrix; $p = 7$ being the total number of parameters specified for water flow modeling in this study (see model specification in Section 2.2.1). The prior mean vector was set to $m_0 = (\hat{y}_h, 0, 0, 0, 0, 0, 0)$, where the level component was set to the average flow value (\hat{y}_h) for hour h (to simply locate the model at the correct scale of the observations) while the remaining components were initiated at 0. The prior variance C_0 is a diagonal p -dimensional matrix with elements equal to 100, which reflect great uncertainty about this prior distribution. In other words, we let the information from the data drive the inference procedure.

The equations that follow describe the evolution distributions. Let $D_t = \{Y_t, D_{t-1}\}$ where D_t denotes the set of information available at time t .

2. Posterior distribution at time $t - 1$

Assume that the posterior distribution of the current state parameters and observational variance at time step $t - 1$ is:

$$\theta_{t-1} | D_{t-1} \sim T_{n_{t-1}}(m_{t-1}, C_{t-1})$$

$$V | D_{t-1} \sim IG\left(\frac{n_{t-1}}{2}, \frac{n_{t-1}S_{t-1}}{2}\right)$$

where, m_{t-1} and C_{t-1} are the posterior location and scale of the state parameter vector (θ_{t-1}) at time $t - 1$. From the system equation, it follows that the prior distribution of the state parameter vector for the next time step t follows a multivariate *Student-t* distribution, that is,

$$\theta_{t-1} | D_{t-1} \sim T_{n_{t-1}}(a_t, R_t),$$

where,

$$a_t = Gm_{t-1} \text{ and } R_t = GC_{t-1}G^T + W_t$$

and W_t is the variance in the evolution error of the system equation and for these equations it is assumed as known. In this study system, W_t is unknown, thus the principle of discount factors was used to estimate the system variance (see below).

3. One-step-ahead forecast

The one-step ahead distribution for water flow at time t follow a *Student-t* distribution, that is,

$$y_t | D_{t-1} \sim T_{n_{t-1}}(f_t, Q_t)$$

which is obtained through Bayes' theorem by combining the prior information at time t with the observation equation, and location f_t and scale Q_t are calculated as follows:

$$f_t = F_t^T a_t$$

$$Q_t = F_t^T R_t F_t + S_{t-1}$$

where F_t is the vector in the observation equation at time t and S_{t-1} is the point estimate of the observational variance from the previous time step $t - 1$.

4. Update

Once a new observation arrives, the posterior distribution of the state vector and the observational variance V is obtained via the Bayes theorem, and it is given by $\theta_t | D_t \sim T_{n_t}(m_t, C_t)$ and $V | D_t \sim IG\left(\frac{n_t}{2}, \frac{n_t S_t}{2}\right)$, where

$$m_t = a_t + A_t e_t$$

$$C_t = \frac{S_t}{S_{t-1}} (R_t - A_t Q_t A_t^T)$$

$$A_t = \frac{R_t F_t}{Q_t}$$

$$n_t = n_{t-1} + 1$$

$$e_t = Y_t - f_t$$

$$S_t = S_{t-1} + \left(\frac{S_{t-1}}{n_t} \right) \left(\frac{e_t^2}{Q_t} - 1 \right),$$

where m_t is the posterior location of the state vector at time t , which is obtained by correcting the prior location (a_t) with a term proportional to e_t , the one-step forward forecast error (i.e., the difference between observed and predicted value), scaled by the adaptive vector A_t , which is a parameter that tunes the forecast error by the relative variances of the prior and likelihood (R_t/Q_t), and the regressor matrix (F_t) (West & Harrison, 1997).

The inferential procedure continues recursively as observations keep arriving. As mentioned earlier, the equations above are valid only if W_t is known. This is rarely the case in practice. One way to estimate the system variance W_t is through stochastic simulations, for example, Markov chain Monte Carlo (MCMC) methods, which are computationally demanding. To avoid this issue, the system variance was approximated with the principle of discount factors (Migon & Alves, 2013). This approach greatly increases the speed of the inference procedure, which is a necessary condition for on-line monitoring algorithms such as in the case of water network monitoring. The variance in the system equation represents the uncertainty in the process over time. In other words, a loss of information across time steps. The discount factor, $0 < \delta \leq 1$, represents, in a subjective way, the percentage of information that is retained from time $t-1$ to time t . For instance, if δ is set to 0.95, it means that 95% of the information is retained from one time step to the next. In practice, high discount factors give more weight to the model priors whereas lower values will give more weight to the new observation (i.e., the likelihood function) when updating model parameters (West & Harrison, 1997). Specifically, under the discount factor approach, W_t is calculated as follows:

$$W_t = \left(\frac{1}{\delta} - 1 \right) C_{t-1} \text{ with } R_t = \frac{(G_t C_{t-1} G_t^T)}{\delta}$$

While the choice of δ is subjective, it is typically set between 0.90 and 0.99 (West & Harrison, 1997). The discount factor value was chosen after fitting the model using 20 different values between 0.90 and 0.995 with increments of 0.005. For each discount factor value, 24 separate daily models for each hour were fitted. Then, the one-step-ahead predictions from these 24 separate models were collapsed and the model root-mean-square error (RMSE) was computed for the dates between 01 March 2015 and 31 December 2016 as follows:

$$\text{RMSE} = \sqrt{\sum_{t=1}^T \sum_{h=1}^m \frac{(y_{h,t} - f_{h,t})^2}{Tm}}$$

where $y_{h,t}$ and $f_{h,t}$ are the observed and predicted flow at hour h and day t , respectively while m is the total number of hours ($m = 24$) and T the total number of days. The DLM with the discount factor (δ) that presented the lowest RMSE value (see Table S1 in Supporting Information S2) was selected to apply the model monitoring tool for break detection.

2.2.3. Estimating Missing Values

Flow readings that are unrecorded due to communication issues between sensors and data loggers (i.e., missing values) are naturally accounted for by the Bayesian framework: no new information leads to no updating of the model parameters (West & Harrison, 1997). In other words, the information set at time t is simply $D_t = D_{t-1}$, the posterior distribution of the state parameters is equal to their priors, that is, $m_t = a_t$, $C_t = R_t$ with the estimate of the observational variance $S_t = S_{t-1}$ and degree of freedom $n_t = n_{t-1}$ also remaining unchanged. To verify the accuracy of the estimation of missing values, as well as how long the DLM could go on without any new observations, an experiment was conducted using the time series from DMA1. An iterative process was developed where, at each iteration, 24 hr of observed flow values were removed from the time series (i.e., considered as missing) and the DLM was then used to fit the entire time series and estimate the missing values. This process was repeated 60 times, resulting in a time range of missing values ranging from 1 to 60 days and, at each iteration, the RMSE was calculated for the predictions of these missing values.

2.2.4. Extraction of Coefficients of Model Predictors

The coefficients and the 95% posterior credible intervals for the main predictors included in the model (level, slope, pressure, temperature, auto regressive order 1, weekend dummies) can be easily obtained from the posterior location (m_t) vector and scale (C_t) matrix. Given that the model is dynamic, predictors may have a statistically significant effect during a period and then be not significant subsequently. Here, a predictor will be significant at a given time when the 95% posterior credible intervals do not overlap with the 0 value. This property allows the modeler to obtain insights into what is driving the time series over time.

2.3. Model Monitoring for Pipe Burst Detection

A model monitoring technique was applied to determine when deterioration occurred in the predictive performance of the DLM (Lipowsky et al., 2010; Wang, Ni, & Wang, 2020). The general idea is to compare the main model, labeled as M_0 , with an alternative model M_1 , that has a change in one parameter of interest. One common method to perform this comparison in Bayesian inference, and DLMs in particular, is the computation of the Bayes factor (West & Harrison, 1997). When a pipe break occurs in a DMA, it affects the hydraulic variables such as water flow, which tends to increase given that the water is lost to the ground while the water consumption of the DMA remains unchanged (Y. Wu & Liu, 2017). Hence, we built an alternative model, M_1 , by shifting the level of the model M_0 by $+ h$ (i.e., simulating a system where a larger flow is expected, as its the case in pipe burst events). At every time step, the Bayesian DLM estimates a probability density function (PDF) for the next measurement of M_0 and one for M_1 . The Bayes factor H_t is the ratio between the PDF from M_0 ($p_0(y_t | D_{t-1}, M_0)$) and M_1 ($p_1(y_t | D_{t-1}, M_1)$), that is

$$H_t = \frac{p_0(y_t | D_{t-1}, M_0)}{p_1(y_t | D_{t-1}, M_1)}$$

The monitoring process assesses the consistency of the observed values Y_t through standardized one-step ahead forecast errors $e_t = \frac{y_t - f_t}{\sqrt{Q_t}}$. While the predictive distribution in DLMs with unknown observational variances follows a *Student-t* distribution, we can approximate it by a Gaussian distribution given our large sample size. In the case of a Gaussian model, the predictive density for the main model M_0 is:

$$p_0(e_t | D_{t-1}) = (2\pi)^{-1/2} \exp\{-0.5(e_t)^2\},$$

and for the alternative model with a level change where e_t has a non-zero mean $+ h$ is:

$$p_1(e_t | D_{t-1}) = (2\pi)^{-1/2} \exp\{-0.5(e_t - h)^2\}$$

Hence, for any fixed shift h , the Bayes' factor at time t can be calculated as follows:

$$H_t = \frac{p_0(y_t | D_{t-1}, M_0)}{p_1(y_t | D_{t-1}, M_1)} = \exp\{0.5(h^2 - 2he_t)\}.$$

Assume that the goal is to investigate the performance of the model predicting k steps-ahead, for $k = \{2, 3, \dots, t\}$, then the evidence against the model M_0 is accumulated multiplicatively as data is processed, that is,

$$H_t(k) = H_t H_{t-1}(k-1)$$

or additively on the log scale

$$\log[H_t(k)] = \log(H_t) + \log[H_{t-1}(k-1)]$$

Following Jeffreys (1961), and as described in West and Harrison (1997), a log Bayes' factor of 1 indicates evidence in favor of M_0 while -1 suggests M_1 is favored. A log Bayes' factor of 2 or more suggests strong evidence for the main model M_0 , while a value of -2 or less indicates high probability that the observation was derived from M_1 . Finally, a value of 0 indicates no evidence favoring either model. The threshold value for outlier detection was set to $\log(H_{\min}) = -2$. The shift value h was set to 3, which combined with $\log(H_{\min})$ of -2 will lead to indifference between models M_0 and M_1 when $e_t = 1.5$ (roughly the upper 90% point of the forecast distribution) and it indicates strong evidence against M_0 when values of forecast errors (e_t) are as high as 2.5 (roughly the upper 99% point of the forecast distribution).

2.3.1. Monitoring Performance

While the modeling of the flow time series was performed on an hourly basis, the historical break data set from the Peninsula Intermediate South DMA contained information only on the day the break was detected by the water utility. Hence, the model performance on break detection was conducted on a daily temporal scale. Note that the proposed model would be capable of detecting break in a much shorter time if applied on a higher resolution flow data (e.g., 1, 5 min) and if the historical break database contained the time of the break. In summary, the algorithm triggers an alert whenever the log-Bayes' factor is lower than $\log(H_{\min})$. The model assumes that a break is detected if the algorithm triggers the alarm during the 24 hr period of the day the break was reported in the historical data set. We also considered a true positive if the alarms are triggered during the 72 hr previous to this day as breaks sometimes take hours or even days to be detected whereas flow outliers could be flagged earlier by the DLM. A pipe break is assumed to be undetected if no alarm was triggered during this (72 hr + 24 hr = 96 hr) period. The number of days in which alerts were triggered by the algorithm was then compiled and its performance was assessed using the true positive rate (TPR) and false positive rate (FPR):

$$\text{TPR} = \frac{\text{TP}}{\text{TP} + \text{FN}} \times 100\%$$

$$\text{FPR} = \frac{\text{FP}}{\text{FP} + \text{TN}} \times 100\%$$

where TP = true positive, which is the number of pipe bursts that were correctly detected, FN = false negative, which refers to the number of bursts that remained undetected, FP = false positive, which is the number of days where no bursts occurred, but a false alarm was triggered, and TN = true negative, being the number of days without bursts and no false alarm was triggered. These metrics can be represented by a confusion matrix. The goal in any modeling approach is to maximize the values in the diagonal (TP, TN) and minimize the values in the off diagonal (FP, FN) of the confusion matrix. While detecting breaks is the primary goal of any monitoring algorithm in a water distribution network, it is also of interest to minimize the number of false alarms it may trigger. Hence, the monitoring tool was also conducted with other threshold values, in particular, $\log(H_{\min}) = -1.5, -2.5$, or -3 to determine the value that had the best trade-off between the number of breaks detected and the number of false alarms triggered.

To complement this analysis, the detection time for the 16 synthetic scenarios of outliers described in Section 2.1.3 was also analyzed. The detection time was calculated as the number of time steps between the start of burst (i.e., first outlier) and the first outlier flagged by the monitoring tool (see Section 2.3) averaged over all synthetic bursts that were detected.

The DLM was coded using R Statistical software v.4.1 (R Core Team, 2021) and a script to run the model along with the data is available (see Henriques-Silva et al., 2022).

3. Results and Discussion

Before fitting the DLM to the flow time series, a similar model was built to estimate missing values in the pressure data. In this case, the model components were trend, slope, an auto-regressive order 1 (Press_{t-1}), temperature, and dummies for weekend days. The false or missing pressure values (DMA 1: 495, DMA 2: 26, Table 1) were replaced by the estimated values from this DLM, and the model fitted to the flow time series assumed that all pressure measurements were observed. After obtaining the one-step ahead forecast for the 24 individual hourly DLMs, they were combined to produce the flow forecast. The flow DLMs with the lowest RMSE were the ones with a discount factor $\delta = 0.95$ (RMSE = 0.066; Table S2 in Supporting Information S2) and $\delta = 0.98$ (RMSE = 0.1254; Table S2 in Supporting Information S2) for DMAs 1 and 2, respectively, and were kept for break detection. The model properties discussed below are illustrated using the results obtained from the DMA 1.

The results for a 1-week period (08 April 2015 to 14 April 2015) are presented in Figure 4a, with the depiction of the observed flow (white circles), one-step ahead forecast (red line), and 95% credible intervals (blue shaded area).

3.1. Estimation of Missing Values

The DLM did a good job capturing the structure of the flow time series. Even during periods with missing observation, the temporal structure was maintained (Figure 4b). For instance, the longest sequences of missing

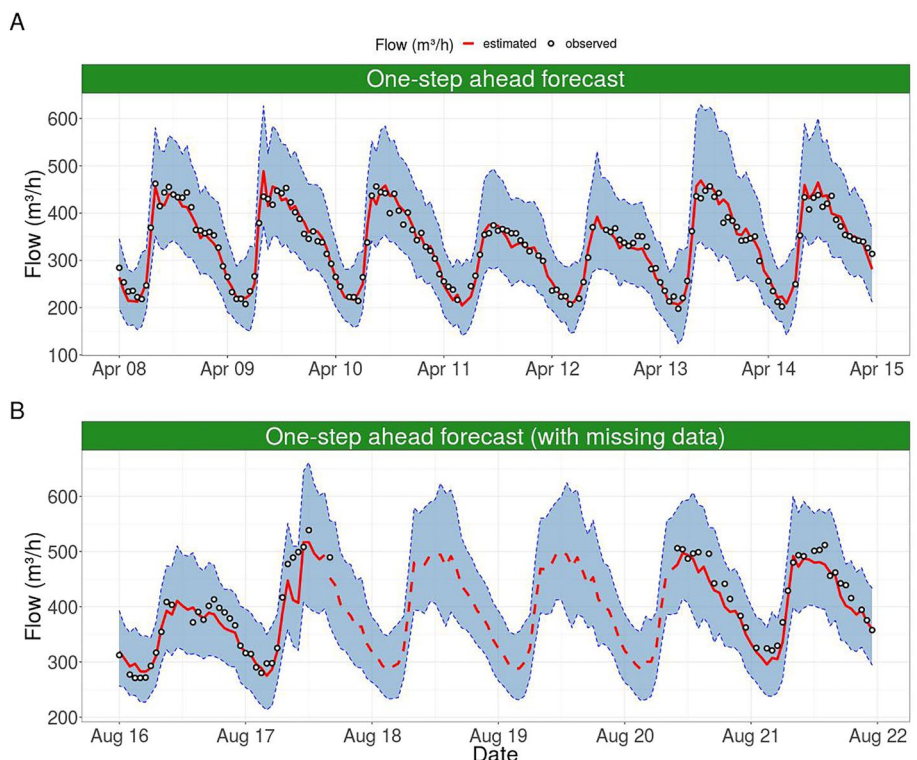


Figure 4. Illustration of one-step ahead forecast of water flow for a period with all flow observations recorded (a) and an example for a period with missing data (b). White circles are the observed hourly flow measurements, the red solid line is the model estimate and the blue shaded area is the limits of the 95% posterior credible intervals.

values occurred in August 2015, where 68 hr passed without valid flow observations. Yet the DLM was able to maintain reasonable predictions (dashed line; Figure 4b). The experiment conducted on accuracy and time-range of the DLM prediction on missing values showed that predictions became less reliable with longer sequences of unrecorded flow measurements (Figure 5). After 30 days of missing flow values (Figure S3 in Supporting Information S1), the predictions of the model became less reliable and the uncertainty increased, as can be noted in the wider credible intervals of the flow predictions between 45 and 60 days of missing values (Figure S3b in Supporting Information S1). Nevertheless, the model predictions were shown to be reasonable for a time-range of at least 15 days (Figure S2a in Supporting Information S1). More specifically, the RMSE varied between 16.1 and 22.9 m³/hr, representing only between 4.9% and 6.5% of the average observed flow of 1–15 days, respectively. This property is desirable given the frequent operational problems in hydraulic sensors and data loggers (Quevedo et al., 2010). After the problem is resolved, because of the recursive nature of the fitting procedure, the model updates its parameters as new observations arrive and provides forecasts for the water flow, without having to learn all over again from the data.

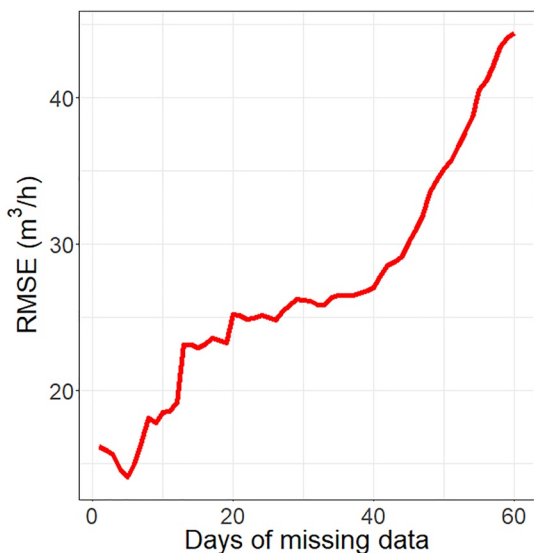


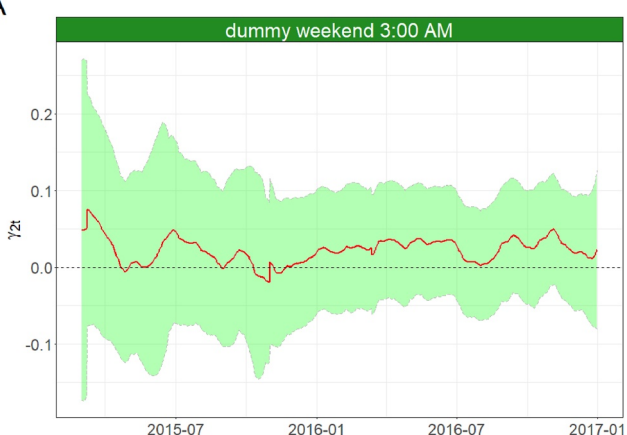
Figure 5. Root-mean squared error (RMSE) calculated at each iteration of the missing value experiment (described in Section 2.2.3), from 1 to 60 days of missing data.

3.2. Effects of Predictors on Estimation of Flow Time Series

The coefficient (red solid line) and 95% credible intervals (green shaded area) for the second weekend dummy variable (γ_2) covering the period of 01 March 2015–31 December 2016 are shown in Figure 6.

To ease the visualization, only the DLMs from two specific hours are depicted: in the top panel (Figure 6a) the coefficient of the dummy variable

A



B

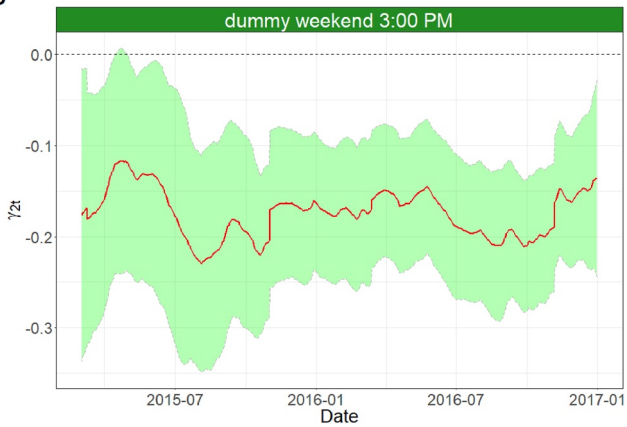


Figure 6. Posterior mean (red solid line) value and 95% posterior credible intervals (green shaded area) for the weekend dummy coefficient (γ_2) from Mars 2015 to December 2016 for the DLMs at 3:00 a.m. (a) and 3:00 p.m. (b).

for the DLM at 3:00 a.m. and in the bottom panel the coefficient for the DLM at 3:00 p.m. (Figure 6b). Clearly, the coefficient for the 3:00 a.m. model rovers around zero for the entire period (Figure 6a), and the 0 value (black dashed line) is always within the posterior credible intervals. This means that there is no association between this variable and the water flow at 3:00 a.m. In contrast, the coefficient for this weekend dummy for the 3:00 p.m. model does not include zero most of the time from July 2015 until the end of the time series (Figure 6b). This is evidenced by the 0 dashed line being outside the 95% posterior credible intervals for most of this period. Note that the coefficient is negative, meaning that during the weekend the predicted water flow decreases (Figure 6b) by around 0.16 units in the log-scale when all the other variables are kept fixed. This is explained by the lower water consumption during weekends compared to workdays, which can be seen in other figures (for instance 11 and 12 April in Figure 1c or Figure 4a). Another example is displayed in Figure 7 where the posterior mean coefficient of temperature was overlayed with actual hourly temperatures for the DLM at 4:00 p.m. It can be observed that there are 2 days (17 June and 13 July) when the air temperature is much higher than the previous day (highlighted by the dashed rectangles; Figure 6). During these days (and the following) the temperature posterior mean coefficient becomes significant in the model, as the 95% credible intervals do not overlap zero. Water demand tends to increase during hot summer days and consequently, water flow in the system increases. Hence the positive effect of the temperature coefficient in the DLM. By taking into account the seasonal effects of temperature in the DLM, the monitoring tool is not affected by it and, in this case, avoids triggering false alarms from the increased water flow in the system.

These examples illustrate an advantage of DLMs, in which coefficients of the model are more easily interpretable compared to complex “black box” algorithms such as neural networks. This feature allows engineers from water utilities to better understand the behavior of the model when forecasting water flow in municipalities; and to naturally include known structures that are related with the flow in the observation equation. To visualize the

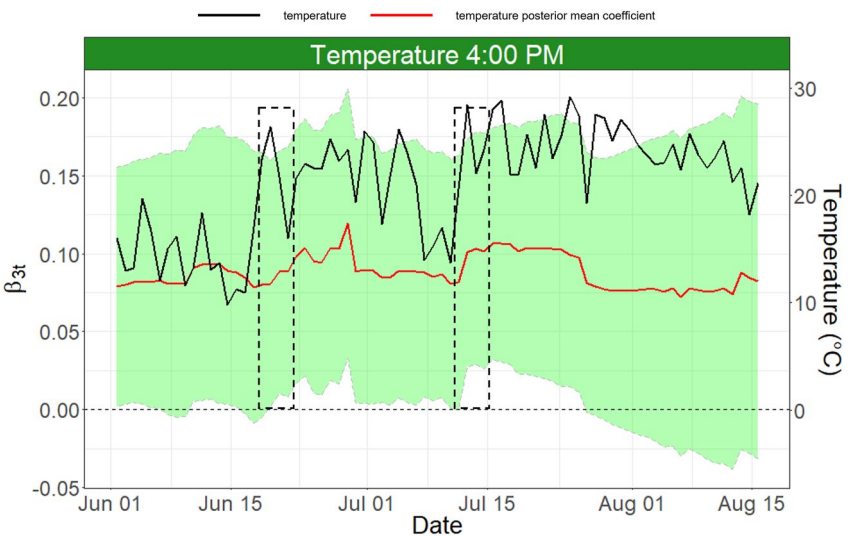


Figure 7. Posterior mean value (red line) and 95% posterior credible intervals (green shaded area) for the temperature coefficient (β_{3t}) from 1st June to 15 August 2016 for the DLMs at 4:00 p.m. (a). The black line represents the air temperature at 4:00 p.m. during this period. The dashed rectangles highlight a large increase in air temperature between 2 days.

Table 2

Confusion Matrix With Results Obtained From Dynamic Linear Model With the Threshold $\log(H_{min})$ Set to -2

	Days with breaks	Days with no breaks
DMA 1		
Alarm triggered	6	44
Alarm not triggered	2	596
DMA 2		
Alarm triggered	20	73
Alarm not triggered	8	510

Note. For rates in percentages, see Table 3.

coefficients for all model components for the DLM, the reader is referred to Figure S1 in Supporting Information S1. For illustrative purposes, instead of 3:00 a.m./p.m. from the example above, a different hour (8:00 a.m.) was chosen. The same negative coefficient for the weekend dummy (Figure S1f in Supporting Information S1) can be seen while the workday dummy is mostly not significant for the entire time series (zero is inside the 95% posterior credible intervals; Figure S1e in Supporting Information S1). Other model components that show a significant effect are pressure, during some periods (Figure S1d in Supporting Information S1), and the model level for the entire time series (Figure S1a in Supporting Information S1).

3.3. Monitoring Tool and Pipe Burst Detection

The results from the model monitoring tool are presented using the threshold for the log Bayes-factor as $\log(H_{min}) = -2$. For DMA 1 (DMA 2), from the 8 (28) historical breaks recorded during the period from March 2015 to December 2016, the model was able to detect 6 (20) (Table 2), having a 75% (71.4%) TPR (Table 3). Out of the 664 (583) days without breaks, the model triggered 44 (73) times (Table 2), resulting in an FPR of ~6.8% (12.5%) (Table 3).

The model monitoring tool did not perform as well on the second, larger, DMA, especially regarding false alarms. Having both inlets and outlets means that the water flow in the pipe network may be influenced by events happening in areas both upstream and downstream of the focal DMA. Hence, outliers that are not related to pipe bursts are more frequent. While some frameworks of outlier classification have been proposed in other methods (Y. Wu et al., 2016; Z. Y. Wu & He, 2021), to the best of our knowledge, there are no such frameworks in DLMs. Nevertheless, in a real-life situation water utility engineers may be aware of events happening in other connected regions to be able to discard false alarms triggered in the focal DMA. This external information can be easily accommodated in the approach proposed here.

In Figure 8, an example of each case from the confusion matrix (see Section 2.2.4) is presented for DMA 1, except for the true negative case. In the top panels, the results from the one-step ahead forecast are presented (Figures 8a, 8c, and 8e) while the bottom panel shows the monitoring tool using Bayes' factor (Figures 8b, 8d, and 8f). For instance, Figure 8a (true positive) shows the flow measurements, the one step-ahead forecast and the 95% posterior credible intervals from 10 to 23 September 2016. The shaded area on the 16 September indicates the day of the pipe burst. At 5:00 a.m., there is an outlier represented by an unusual flow peak in the time series that is flagged by the monitoring tool (Figure 8b) when the $\log(H_t)$ metric falls well below the -2 threshold (horizontal red dashed line). An example of an undetected pipe break is illustrated in Figure 8c. The break was reported on 26 January 2016 and is highlighted with the shaded area in the top panel. In this case, the Bayes factor metric did not drop below the threshold (Figure 8d). It is possible that this event was a small burst, which induced an increase in flow that may be too small relative to the total flow of the DMA and hence not distinguishable from natural random flow patterns. A similar display was created for DMA 2 (Figure 9):

In May 2016, a break was reported on the 6th in the historical break data set. However, abnormal flow values started on the evening of 4 May 2016 and especially on the night of 5 May 2016, where the minimum night flow was way above flow values from the previous nights (Figure 9a). The alarm triggered for all flow measurements during 5 May (Figure 9b) and in a few instances during 6 May, suggesting that it was a large break. In panels c and d of Figure 9, a pipe break that occurred on the 20 April 2015 was not detected by the model. While the morning flow values on the two previous days were higher than normal (Figure 9d), they were not large enough to be above the upper confidence interval, hence no alarm was triggered.

The DLM break monitoring tool also triggered some false positives (i.e., alarm triggered but without any break; Tables 2 and 3). For instance, Figure 8e depicts one of these situations where there were a few spikes in water flow at night on 14 October while no break was recorded that day in DMA 1. The monitoring tool detected them when $\log(H_t)$ crossed the

Table 3

Sensitivity Analysis With Different Threshold Values for the Log-Bayes Factor ($\log(H_{min})$)

DMA	$\log(H_{min})$	TPR	FPR
1	-1.5	75%	8.9%
1	-2.0	75%	6.88%
1	-2.5	75%	5.15%
1	-3.0	62.5%	3.9%
2	-1.5	78.6%	23.32%
2	-2.0	71.4%	12.52%
2	-2.5	53.57%	10.97%
2	-3.0	46.43%	9.1%

Note. TPR, true positive rate; FPR, false positive rate.

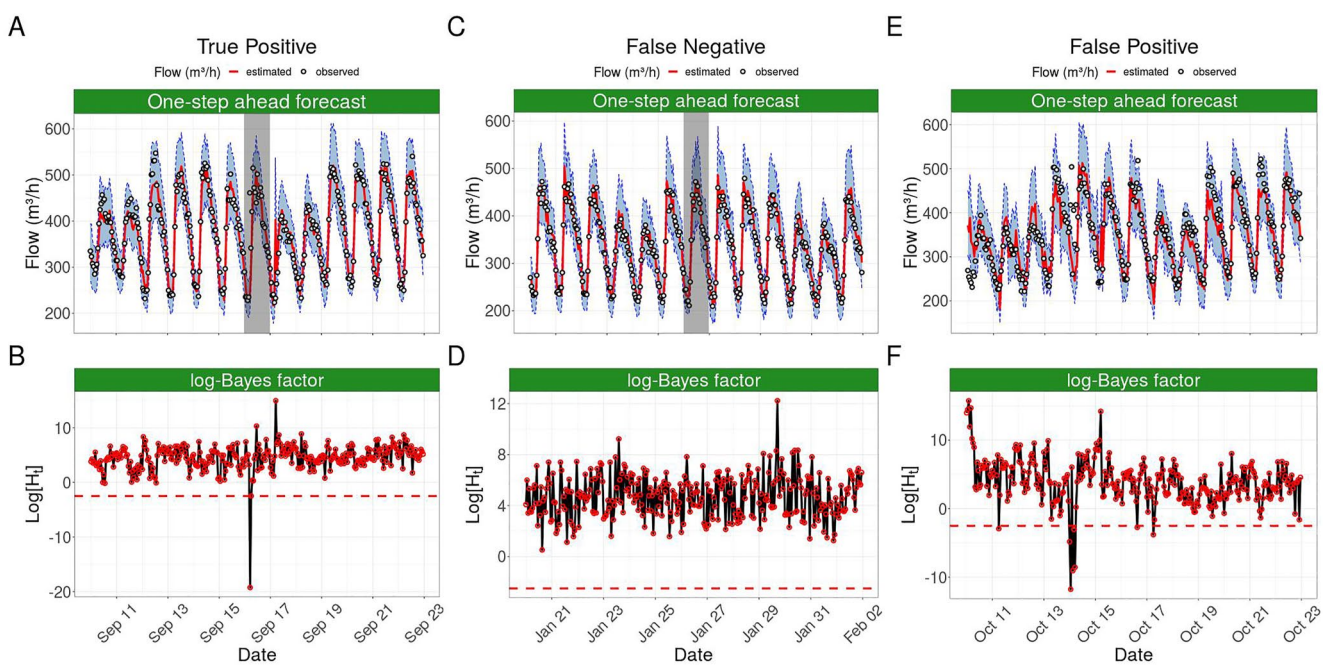


Figure 8. Examples of true positive (a, b), false negative (c, d) and false positive (e, f) in DMA 1. The top panels depict the one-step ahead forecast of water flow. White circles are the observed hourly flow measurements, the red solid line is the model estimate and the blue shade around the line is the 95% posterior credible intervals. The gray shaded area represents the day in which a pipe burst occurred. The bottom panels show the computation of the log-Bayes factor at each time step. The threshold $\log(H_{\min})$ is represented by the horizontal red dashed line. Note that the x-axis labels from the top panels were removed for better readability but they are the same than the bottom ones.

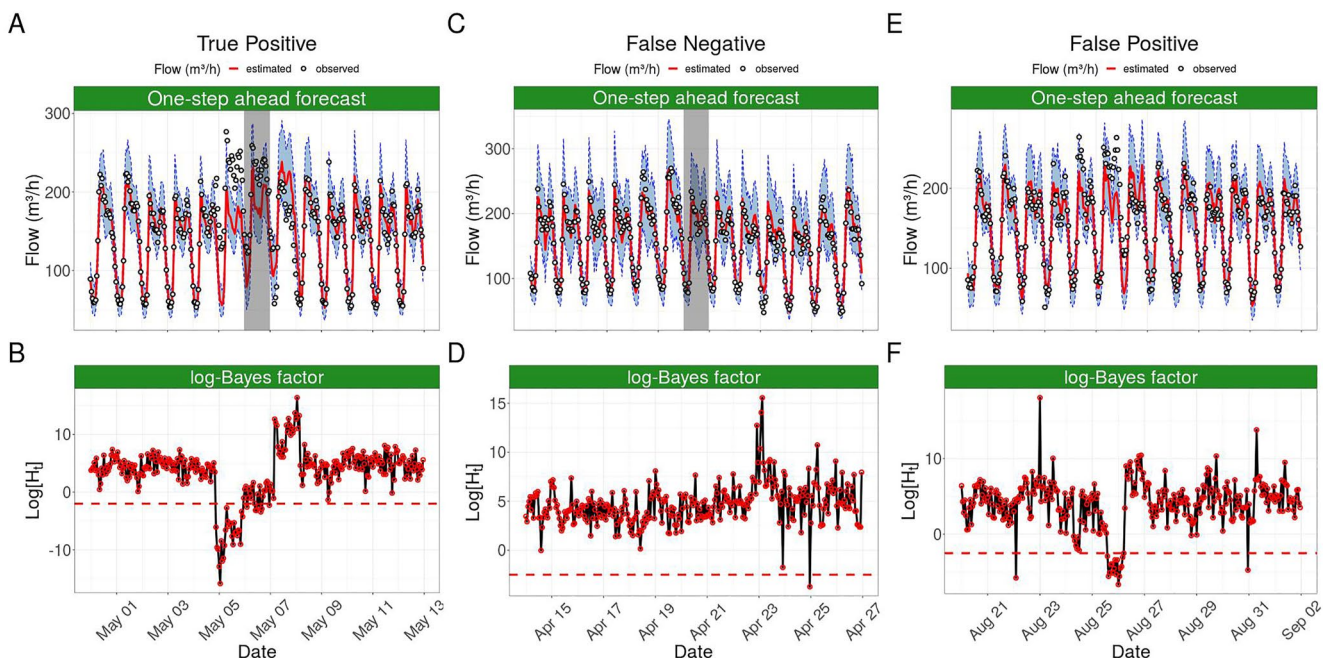


Figure 9. Examples of true positive (a, b), false negative (c, d), and false positive (e, f) in DMA 2. The top panels depict the one-step ahead forecast of water flow. White circles are the observed hourly flow measurements, the red solid line is the model estimate and the blue shade around the line is the 95% posterior credible intervals. The gray shaded area represents the day in which a pipe burst occurred. The bottom panels show the computation of the log-Bayes factor at each time step. The threshold $\log(H_{\min})$ is represented by the horizontal red dashed line. Note that the x-axis labels from the top panels were removed for better readability but they are the same than the bottom ones.

Table 4

Results for the Synthetic Burst Experiment Using a Level Shift Value (h) Equal to 3 (See Section 2.3 in the Methods for More Details)

Scenario	Starting timestamp	Burst size	Detection time	Detected bursts	FPR
1	2:00 a.m.	8%	3.36	14/30	5.97%
2	2:00 a.m.	10%	2.85	20/30	5.96%
3	2:00 a.m.	12%	2	23/30	5.95%
4	2:00 a.m.	15%	1.57	23/30	5.95%
5	8:00 a.m.	8%	5.5	6/30	5.95%
6	8:00 a.m.	10%	5.78	9/30	5.95%
7	8:00 a.m.	12%	4.8	11/30	5.95%
8	8:00 a.m.	15%	3.29	17/30	5.95%
9	2:00 p.m.	8%	4.2	5/30	5.97%
10	2:00 p.m.	10%	4.44	9/30	5.97%
11	2:00 p.m.	12%	5.21	14/30	5.97%
12	2:00 p.m.	15%	3.25	20/30	5.97%
13	8:00 p.m.	8%	6.55	11/30	6.01%
14	8:00 p.m.	10%	6.14	14/30	6.01%
15	8:00 p.m.	12%	4.61	23/30	6.03%
16	8:00 p.m.	15%	3.56	27/30	6.06%

Note. Each row represents a different scenario. Starting timestamp represents the timestamp when each burst started; burst size is measured as a percentage of the average daily flow from the day the burst occurred; detection time is measured as the number of time steps between the start of the burst and when the first outlier was flagged by the monitoring tool averaged over all detected pipe bursts; detected bursts is the number of synthetic bursts that were detected from the 30 that were simulated. The FPR is the false positive rate.

threshold (red dashed line; Figure 8f), and while these spikes were not related to a pipe burst, another event might have occurred that made the DMA water flow at night jump to as much as 500 m³/hr. A similar situation occurred on 26 August 2016 in DMA2 (Figure 9e) where $\log(H_i)$ values remained most of the day below the threshold (Figure 9f). It is important to highlight that such deviations might still be of interest to the engineers from the water utility. False positives can occur due to illegal connections, unexpected water usages, large events occurring in the city, pipe flushing or sensor failures (Romano et al., 2014). DLMs allow for model intervention to incorporate change-point information if particular events that will affect the system are known in advance (West & Harrison, 1997). Model intervention may take form in increasing the variance of model parameters, which reflects the increasing uncertainty about the future, or by decreasing the discount factor (δ) to better accommodate new observations following these potential changes (West & Harrison, 1997). Others have proposed dummy variables indicating change-point events (Jiang et al., 2007) such as, for instance, closing a valve in the water distribution network (Jung & Lansey, 2015). While beyond the scope of this study, these approaches could be utilized by water utilities to inform the model about, for instance, pipe flushing events.

Changing the threshold values for the Bayes factor mainly affected the FPR, going from around 8.9% when $\log(H_{\min})$ was set to -1.5 down to 3.9% when it was set to -3 (Table 3) in DMA 1. Break detection was not affected by the threshold in DMA 1, where only using the most conservative value of $\log(H_{\min}) = -3$ an additional pipe break became undetected (Table 3). The best trade-off between break detection and the minimization of false positives was with $\log(H_{\min}) = -2.5$, where break detection remained similar to larger threshold values (-1.5 and -2) but with a lower FPR (5.15%; Table 3). Changing the threshold values for the DLM in the second DMA had more impact. The FPR halved between $\log(H_{\min}) = -1.5$ and -2 (from 23% to 12%) and then decreased to around 9% for the most conservative threshold ($\log(H_{\min}) = -3$). Likewise, the detection rate went from 78% on the threshold $\log(H_{\min}) = -1.5$ to about 46% using the more conservative threshold ($\log(H_{\min}) = -3$; Table 3).

In this case, the best trade-off between break detection and the minimization of false positives was when $\log(H_{\min}) = -2$, where break detection remained high (71%) and the FPR was halved compared to $\log(H_{\min}) = -1.5$. Changing the threshold to -2.5 would greatly reduce detection rate to 53% while not significantly changing the FPR (10% instead of 12%; Table 3).

The optimal threshold value will depend on both the problem at hand and the data available. If it is important to keep the FPR to a minimum, a more conservative threshold (i.e., smaller $\log(H_{\min})$) is recommended. Conversely, if maximizing TPR is primordial, then a larger $\log(H_{\min})$ can be used. The choice is up to the decision maker using the model and the DLM is fast enough to run (see Conclusion) for a comprehensive sensitivity analysis of model parameters to be estimated in order to select the optimal parameter values to tackle the problem at hand.

3.4. Detection Time

The synthetic burst experiment evidenced that the DLM showed a reasonable detection time in most of the scenarios that were tested (Table 4). For this experiment, a threshold $\log(H_{\min}) = -2$ was used. The lowest average detection time measured was only 1.57 hr for a large burst starting at 2:00 a.m. (scenario 4) up to 6.55 hr, on average, for the scenario 13 (small burst starting at 8:00 p.m.; Table 4). As expected, the fastest detection time was measured for bursts starting at 02:00 a.m. when water demand is at its lowest (Table 4). Likewise, the larger the burst was, the fastest it was detected as shown by shorter detection times for burst sizes of 15% compared to ones at 8%. The FPR for these scenarios was around 5.9% (Table 4). We also tested the same scenarios but using a lower-level shift ($h = 2$), meaning that the monitoring tool would be more sensitive to smaller deviations between observed and expected flow values (Table S2 in Supporting Information S2). The number of detected breaks

and the average detection time was improved for all tested scenarios compared to the ones presented in Table 4. More specifically, lowering the mean level for alternative model (M_1), the monitoring tool was able to detect 30% more small breaks (breaks simulated by increasing the average daily inflow by 8% or 10%), while the detection time improved only marginally (2% lower detection time). For larger breaks, that is, simulated by increasing the average daily inflow by 12% or 15%, the detection time decreased by 7% and 9% respectively, and the number of detected breaks increased by 10% and 17%, respectively. This came at a cost of a higher FPR, although by not much (FPR $\sim 5.9\%$ with $h = 3$ and FPR $\sim 7.35\%$ with $h = 2$ for all scenarios; Table 4, Table S2 in Supporting Information S2). Similar to the threshold for the Bayes factor, the value of the level shift (h) can be chosen by decision makers to meet their needs while having in mind that there is a trade-off between the ability of the model to detect more breaks and the amount of the false positives it will generate.

Note that the detection time is measured in hours because the DLM was fitted with hourly data. Hence, in our case, the detection time can never be lower than 1 hr as this is the minimum time unit. However, detection time is measured as the number of time steps it takes for the alarm to be triggered after the break occurred, time step being the frequency on which observations are measured. If the flow data is at 5 or 15 min frequency, the threshold of the monitoring tool will be tested every 5 or 15 min, respectively. Likewise, if the flow data is one an hourly scale, such as in our simulation, the threshold will be tested every hour. Hence, if the present model was applied to a time series at finer resolutions (e.g., 5, 15 min), the detection time could probably be much faster if outliers were to be flagged within periods shorter than 1 hour, being on par with the detection time of state-of-the art deep learning algorithms (e.g., Wang et al., 2020). Such endeavor is outside of the scope of this study as a new DLM structure would be required to model a different temporal scale, with other seasonal/cyclical factors, finer-scale resolution for external predictors and so on. Future studies could conduct a more thorough analysis to evaluate the detection time of DLMs under different temporal scales of water flow in order to validate this premise.

3.5. Limitations

One of the challenges in DLM's is the estimation of the covariance matrix of the evolution equation W . In this study, discount factors were used to avoid its direct estimation. As results can be sensitive to the choice of the discount factors, a sensitivity analysis was proposed to choose the most appropriate value (Table S1 in Supporting Information S2). Given that the algorithm runs fast, the sensitivity analysis should not be a major issue. One way to improve this is to make the covariance matrix W unknown and use MCMC methods to obtain samples from the resultant posterior distribution. Given that MCMC is computationally intensive, the use of Forward filtering Backward Sampling algorithm is recommended when sampling from the posterior full conditional of the state vector. See for example, Schmidt and Lopes (2019) for a review of the algorithm.

Another limitation of the proposed algorithm is that it cannot pinpoint the exact location of a pipe burst in the DMA. Identifying which flowmeter in the water distribution network is recording the most flow outliers can help reduce the search area. Using the time series from multiple flow meters spatially spread across the DMA could be used to develop more complex spatio-temporal Bayesian models that could be used to not only detect the presence of bursts but also their potential location.

Finally, the methodology presented here is based on the decomposition of the time-series into separate 24 DLMs, one for each hour of the day. To apply the same methodology to finer resolution data means increasing the number of DLMs to be fitted (e.g., 48 DLMs for 30 min intervals, 96 DLMs for 15 min intervals and so on). While this may improve the detection time of pipe burst, it will inevitably increase the computation time to run the model (see Conclusion). Hence, the end-user needs to have this trade-off in mind and select the minimum necessary timescale for the data to properly tackle the problem at hand. Another issue is that the modeler will need to measure the necessary covariates at the same finer timescales, which sometimes is not practical.

4. Conclusion

The implementation of SCADA systems in water distribution network worldwide have bolstered the development of monitoring algorithms to use real-time flow and/or pressure data in order to detect pipe bursts as quickly as possible (Romano et al., 2014; Ye & Fenner, 2011; Zhou et al., 2019) for early intervention. A novel methodology for burst detection using Bayesian forecasting and DLM integrated with a model monitoring tool has been developed in this study. The model is extremely fast and took only 1.8 s on an ASUS VivoBook laptop (Intel Core

i5-8250U CPU, 8Mb RAM) to run on the almost 2 yr of hourly flow time-series (i.e., 17,400 observations). This makes it a viable option for real-time water distribution network monitoring. The DLM enables the modeling of a time-dependent variable by incorporating different components such as trends, seasonality, and regression effects. The present study has demonstrated that DLMs can capture well the structure of flow time series in water distribution networks. Indeed, water flow is correlated with water consumption in municipalities, which is known to be influenced by many factors (e.g., temperature, precipitation, large events) and present periodicity such as daily, weekly, and yearly seasonality. Different municipalities and/or DMAs may have idiosyncrasies that affect the flow time series. Hence, it is suggested a careful analysis of the flow time series together with inputs and feedbacks from water engineers responsible for the water distribution network to implement the proposed model to a given DMA. Nevertheless, the model is very flexible and able to accommodate these different features. Modelers can easily add new regressors if required and use model intervention techniques (see Discussion section for some suggested techniques) to account for punctual events. Further, the monitoring tool is flexible, allowing for end-users to decide the best threshold to minimize the number of false alarms and maximize the number of detected breaks. Moreover, DLMs do not break down when flow measurements are unrecorded (i.e., missing), and allow for model intervention in cases of known events that may change system behavior, two properties that are essential when dealing with a water distribution network operation.

Data Availability Statement

The data set along with an R script to run the model used in this study is available at https://data.4tu.nl/articles/dataset/Data_underlying_the_research_on_On-line_warning_system_for_pipe_burst_using_Bayesian_dynamic_linear_models/17169383 for download (Henriques-Silva et al., 2022).

Acknowledgments

The authors are grateful to John Eismor and Kevin Healy from Halifax Water for providing the water flow and historical breaks data sets. The authors are thankful to Jack Sklivas for helping to create the DMA maps, and to Helio S. Migon and Larissa C. Alves for sharing their R Script with the Kalman filtering equations. This study was funded by the Mitacs Accelerate Program (<https://www.mitacs.ca/en/programs/accelerate>; Grant IT15343) with matching funds from CANN Forecast (<https://www.cannforecast.com/>).

References

- Bakker, M., Vreeburg, J. H. G., Van De Roer, M., & Rietveld, L. C. (2014). Heuristic burst detection method using flow and pressure measurements. *Journal of Hydroinformatics*, 16(5), 1194–1209. <https://doi.org/10.2166/hydro.2014.120>
- Ciupak, M., Ozga-Zielinski, B., Adamowski, J., Quilty, J., & Khalil, B. (2015). The application of dynamic linear Bayesian models in hydrological forecasting: Varying coefficient regression and discount weighted regression. *Journal of Hydrology*, 530, 762–784. <https://doi.org/10.1016/j.jhydrol.2015.10.023>
- Folkman, S. (2018). *Water main break rates in the USA and Canada: A comprehensive study*. Utah State University Buried Structures Laboratory.
- Geelen, V. C. C., Yntema, D. R., Molenaar, J., & Keesman, K. J. (2019). Monitoring support for water distribution systems based on pressure sensor data. *Water Resources Management*, 33(10), 3339–3353. <https://doi.org/10.1007/s11269-019-02245-4>
- Henriques-Silva, R., Schmidt, A. M., Saran, N., Duchesne, S., & St-Gelais, N. F. (2022). Data underlying the research on on-line warning system for pipe burst using Bayesian dynamic linear models (Version 1) [Dataset]. 4TU.ResearchData. <https://doi.org/10.4121/17169383.v1>
- Hu, Z., Chen, B., Chen, W., Tan, D., & Shen, D. (2021). Review of model-based and data-driven approaches for leak detection and location in water distribution systems. *Water Supply*, 21(7), 3282–3306. <https://doi.org/10.2166/ws.2021.101>
- Jeffreys, H. (1961). *Theory of probability* (3rd ed.). Oxford Clarendon Press.
- Jian, C., Gao, J., & Xu, Y. (2022). Anomaly detection and classification in water distribution networks integrated with hourly nodal water demand forecasting models and feature extraction technique. *Journal of Water Resources Planning and Management*, 148(11), 04022059. [https://doi.org/10.1061/\(ASCE\)WR.1943-5452.0001616](https://doi.org/10.1061/(ASCE)WR.1943-5452.0001616)
- Jiang, W., Au, T., & Tsui, K.-L. (2007). A statistical process control approach to business activity monitoring. *IIE Transactions*, 39(3), 235–249. <https://doi.org/10.1080/07408170600743912>
- Jung, D., & Lansey, K. (2015). Water distribution system burst detection using a nonlinear Kalman filter. *Journal of Water Resources Planning and Management*, 141(5), 04014070. [https://doi.org/10.1061/\(ASCE\)WR.1943-5452.0000464](https://doi.org/10.1061/(ASCE)WR.1943-5452.0000464)
- Kingdon, B., Liemberger, R., & Marin, P. (2006). *The challenge of reducing Non-Revenue Water (NRW) in developing countries (water supply and sanitation sector board discussion paper series, 8)*. The World Bank. Retrieved from <http://siteresources.worldbank.org/INTWSS/Resources/WSS8fin4.pdf>
- Li, R., Huang, H., Xin, K., & Tao, T. (2015). A review of methods for burst/leakage detection and location in water distribution systems. *Water Supply*, 15(3), 429–441. <https://doi.org/10.2166/ws.2014.131>
- Lipowsky, H., Staudacher, S., Bauer, M., & Schmidt, K.-J. (2010). Application of Bayesian forecasting to change detection and prognosis of gas turbine performance. *Journal of Engineering for Gas Turbines & Power*, 132(3), 031602. <https://doi.org/10.1115/1.3159367>
- Liu, Y., & Fan, X. (2020). Bayesian prediction of bridge extreme stresses based on DLTM and monitoring coupled data. *Structural Health Monitoring*, 19(20), 454–462. <https://doi.org/10.1177/1475921719853171>
- Ma, X., Li, Y., Zhang, W., Li, X., Shi, Z., Yu, J., et al. (2022). A real-time method to detect the leakage location in urban water distribution networks. *Journal of Water Resources Planning and Management*, 148(2), 04022069. [https://doi.org/10.1061/\(ASCE\)WR.1943-5452.0001628](https://doi.org/10.1061/(ASCE)WR.1943-5452.0001628)
- Migon, H. S., & Alves, L. C. (2013). Multivariate dynamic regression: Modeling and forecasting for intraday electricity load. *Applied Stochastic Models in Business and Industry*, 29(6), 579–598. <https://doi.org/10.1002/asmb.1990>
- Mounce, S. R., Boxal, J. B., & Machell, J. (2010). Development and verification of an online artificial intelligence system for burst detection in water distribution systems. *Journal of Water Resource Planning and Management*, 136(3), 309–318. [https://doi.org/10.1061/\(ASCE\)WR.1943-5452.0000030](https://doi.org/10.1061/(ASCE)WR.1943-5452.0000030)
- Mounce, S. R., Day, A. J., Wood, A. S., Khan, A., Widdop, P. D., & Machell, J. (2002). A neural network approach to burst detection. *Water Science and Technology*, 45(4–5), 237–246. <https://doi.org/10.2166/wst.2002.0595>

- Mounce, S. R., Mounce, R. B., & Boxall, J. B. (2011). Novelty detection for time series data analysis in water distribution systems using support vector machines. *Journal of Hydroinformatics*, 13(4), 672–686. <https://doi.org/10.2166/hydro.2010.144>
- Nakhkash, M., & Mahmood-Zadeh, M. R. (2004). Water leak detection using ground penetrating radar. Presented at the Tenth International Conference on Ground Penetrating Radar, 21–24 June.
- Navarro-Díaz, A., Delgado-Aguilera, J. A., Santos-Ruiz, I., & Puig, V. (2022). Real-time leak diagnosis in water distribution systems based on a bank of observers and genetic algorithm. *Water*, 14(20), 3289. <https://doi.org/10.3390/w14203289>
- Nobre, F. F., Monteiro, A. B. S., Telles, P. R., & Williamson, G. D. (2001). Dynamic linear model and SARIMA: A comparison of their forecasting performance in epidemiology. *Statistics in Medicine*, 20(20), 3051–3069. <https://doi.org/10.1002/sim.963>
- Petris, G., Petrone, S., & Campagnoli, P. (2009). *Dynamic linear models with R*. Springer.
- Pole, A., West, M., & Harrison, P. J. (1994). *Applied Bayesian forecasting and time series analysis*. Chapman-Hall.
- Puust, R., Kapelan, Z., Savic, D. A., & Koppel, T. (2010). A review of methods for leakage management in pipe networks. *Urban Water Journal*, 7(1), 25–45. <https://doi.org/10.1080/15730621003610878>
- Quevedo, J., Puig, V., Cembrano, G., Blanch, J., Aguilar, J., Saporta, D., et al. (2010). Validation and reconstruction of flow meter data in the Barcelona water distribution network. *Control Engineering Practice*, 18(6), 640–651. <https://doi.org/10.1016/j.conengprac.2010.03.003>
- Ravines, R. R., Schmidt, A. M., Migon, H. S., & Rennó, C. D. (2008). A joint model for rainfall-runoff: The case of Rio Grande Basin. *Journal of Hydrology*, 353(1–2), 189–200. <https://doi.org/10.1016/j.jhydrol.2008.02.008>
- R Core Team. (2021). *R: A language and environment for statistical computing*. R Foundation for Statistical Computing. Retrieved from <https://www.R-project.org/>
- Rezaei, H., Ryan, B., & Stoianov, I. (2015). Pipe failure analysis and impact of dynamic hydraulic conditions in water supply networks. *Procedia Engineering*, 119, 253–262. <https://doi.org/10.1016/j.proeng.2015.08.883>
- Romano, M., Kapelan, Z., & Savić, D. A. (2014). Automated detection of pipe bursts and other events in water distribution systems. *Journal of Water Resources Planning and Management*, 140(4), 457–467. [https://doi.org/10.1061/\(ASCE\)WR.1943-5452.0000339](https://doi.org/10.1061/(ASCE)WR.1943-5452.0000339)
- Sadiq, R., Klenner, Y., & Rajani, B. (2006). Estimating risk of contaminant intrusion in water distribution networks using Dempster-Shafer theory of evidence. *Civil Engineering and Environmental Systems*, 23(3), 129–141. <https://doi.org/10.1080/10286600600789276>
- Schmidt, A. M., & Lopes, H. F. (2019). Dynamic models. In A. E. Gelfand, M. Fuentes, J. Hoeting, & R. Smith (Eds.), *Handbook of environmental and ecological statistics* (pp. 57–80). Chapman & Hall/CRC.
- Wan, X., Kuhaneftani, P. K., Farmani, R., & Keedwell, E. (2022). Literature review of data analytics for leak detection in water distribution networks: A focus on pressure and flow smart sensors. *Journal of Water Resources Planning and Management*, 148(10), 03122002. [https://doi.org/10.1061/\(ASCE\)WR.1943-5452.0001597](https://doi.org/10.1061/(ASCE)WR.1943-5452.0001597)
- Wang, X. T., Guo, G. C., Liu, S. M., Wu, Y. P., Xu, X. Y., & Smith, K. (2020). Burst detection in district metering areas using deep learning method. *Journal of Water Resources Planning and Management*, 146(6), 04020031. [https://doi.org/10.1061/\(ASCE\)WR.1943-5452.0001223](https://doi.org/10.1061/(ASCE)WR.1943-5452.0001223)
- Wang, Y. W., Ni, Y. Q., & Wang, X. (2020). Real-time defect detection of high-speed train wheels by using Bayesian forecasting and dynamic model. *Mechanical Systems and Signal Processing*, 139, 106654. <https://doi.org/10.1016/j.ymssp.2020.106654>
- West, M., & Harrison, J. (1997). *Bayesian forecasting and dynamic models* (2nd ed.). Springer-Verlag.
- Wu, Y., & Liu, S. (2017). A review of data-driven approaches for burst detection in water distribution systems. *Urban Water Journal*, 14(9), 972–983. <https://doi.org/10.1080/1573062X.2017.1279191>
- Wu, Y., Liu, S., Wu, X., Liu, Y., & Guan, Y. (2016). Burst detection in district metering areas using a data-driven clustering algorithm. *Water Research*, 100, 28–37. <https://doi.org/10.1016/j.watres.2016.05.016>
- Wu, Z. Y., & He, Y. (2021). Time series data decomposition-based anomaly detection and evaluation framework for operational management of smart water grid. *Journal of Water Resources Planning and Management*, 147(9), 04021059. [https://doi.org/10.1061/\(ASCE\)WR.1943-5452.0001433](https://doi.org/10.1061/(ASCE)WR.1943-5452.0001433)
- Yamijala, S., Guijema, S. D., & Brumbelow, K. (2009). Statistical models for the analysis of water distribution system pipe break data. *Reliability Engineering & System Safety*, 94(2), 282–293. <https://doi.org/10.1016/j.ress.2008.03.011>
- Ye, G., & Fenner, R. A. (2011). Kalman filtering of hydraulic measurements for burst detection in water distribution systems. *Journal of Pipeline Systems Engineering and Practice*, 2(1), 14–22. [https://doi.org/10.1061/\(ASCE\)PS.1949-1204.0000070](https://doi.org/10.1061/(ASCE)PS.1949-1204.0000070)
- Ye, G., & Fenner, R. A. (2014). Study of burst alarming and data sampling frequency in water distribution networks. *Journal of Water Resources Planning and Management*, 140(6), 06014001. [https://doi.org/10.1061/\(ASCE\)WR.1943-5452.0000394](https://doi.org/10.1061/(ASCE)WR.1943-5452.0000394)
- Zhou, X., Tang, Z., Xu, W., Meng, F., Chu, X., Xin, K., & Fu, G. (2019). Deep learning identifies accurate burst locations in water distribution networks. *Water Research*, 166, 115058. <https://doi.org/10.1016/j.watres.2019.115058>

Erratum

In the originally published version of this article, the name Sklivas was incorrectly spelled as Skivlas in the second sentence of the Acknowledgments section. This misspelling has been corrected, and this may be considered the authoritative version of record.